

See discussions, stats, and author profiles for this publication at: <https://www.researchgate.net/publication/229100258>

Assessment of density functional methods for the study of vanadium and rhenium complexes with thiolato ligands

ARTICLE *in* JOURNAL OF MOLECULAR STRUCTURE THEOCHEM · FEBRUARY 2010

Impact Factor: 1.37 · DOI: 10.1016/j.theochem.2009.10.020

CITATIONS

30

READS

31

3 AUTHORS, INCLUDING:



Jorge S. Gancheff

University of the Republic, Uruguay

45 PUBLICATIONS 337 CITATIONS

SEE PROFILE



Pablo A. Denis

University of the Republic, Uruguay

104 PUBLICATIONS 1,559 CITATIONS

SEE PROFILE



Assessment of density functional methods for the study of vanadium and rhenium complexes with thiolato ligands

Jorge S. Gancheff^{a,*}, Pablo A. Denis^b, F. Ekkehardt Hahn^a

^a Institut für Anorganische und Analytische Chemie der Westfälischen Wilhelms-Universität Münster, Corrensstrasse 30, 48149 Münster, Germany

^b Computational Nanotechnology, DETEMA, Facultad de Química, Udelar, Montevideo, Uruguay

ARTICLE INFO

Article history:

Received 23 September 2009

Accepted 16 October 2009

Available online 6 November 2009

Keywords:

Thiolato ligands

Oxocomplexes

Rhenium(V)

Vanadium(IV)

DFT methods

ABSTRACT

Herein, we report the assessment of six DFT methods (BP86, TPSS, B3LYP, X3LYP, PBE1PBE, BH&HLYP) in describing the nature of the chemical bonds, structural, and electronic properties of the closed-shell oxocomplex of Re(V) $[\text{ReO}(\text{bdt})_2]^-$ and the open-shell oxocomplex of V(IV) $[\text{VO}(\text{bdt})_2]^{2-}$ ($\text{bdt}^{2-} = 1,2\text{-benzenedithiolato}$). Several basis sets were employed, and different effective core potentials were taken as variables into account. PBE1PBE is found to be the best overall performer in describing M=S bonds. It is followed by two groups composed in turn of BP86, TPSS, and BH&HLYP, and another one including B3LYP and X3LYP. For the M=O bonds, the performance has a direct dependency on the Hartree–Fock exchange. On going from the pure GGA (BP86) and *m*-GGA (TPSS) to BH&HLYP, a sensible improvement is obtained for the Re=O bond distances. However, for the V=O bond the opposite is true, being BH&HLYP the worst choice. The M=S and M=O chemical bonds have been analyzed in terms of the natural bond orbital theory. All sulfur atoms participate in σ bonds strongly polarized toward the non-metal, in which the hybridization at the metal has mainly *d* character and at the non-metal, *p* character. For the Re=O bonds, interesting features were found. This work shows that PBE1PBE in combination with the MIDI! basis set and the Stuttgart energy consistent pseudopotentials for metals is the best methodology for the study of rhenium and vanadium complexes with thiolato ligands. We have tested our hypothesis performing comparative calculations for the $[\text{Re}_6\text{S}_8\text{X}_6]^{4-}$ ($\text{X}^- = \text{Cl}^-, \text{Br}^-, \text{I}^-$) hexanuclear clusters. The results obtained at the PBE1PBE/STMIID significantly improve those published previously and the computational cost is small. Therefore, we recommend this methodology to study large of transition metal complexes containing thiolato ligands.

© 2009 Elsevier B.V. All rights reserved.

1. Introduction

The study of the coordination chemistry of complexes with thiolato ligands has aroused particular interest due to their electrochemistry, photochemistry, and potential applications as, non-linear optical materials, superconductors, compounds with unusual magnetic properties, and bio-catalysts [1–6]. Oxocomplexes of Mo and W containing dithiolato ligands have been extensively studied due to their role in metalloenzyme active sites [7–13]. However, the investigations of those containing other metallic centers, such as V(IV) and Re(V), have not been carried out in the same extension. The electronic structure of the center $\{\text{VOS}_4\}$ in $[\text{VO}(\text{bdt})_2]^{2-}$ ($\text{bdt}^{2-} = 1,2\text{-benzenedithiolato}$) has been studied by Cooney et al. [14], providing valuable background information regarding the mode-of-action of vanadium-containing nitrate reductase (V-NR), analogous to molybdenum-containing bacterial NR. Oxocomplexes of rhenium(V) containing dithiolato ligands

have been attracted attention due to their role in oxygen atom transfer reactions (OAT) [15–17], and because the nuclear properties of ^{186}Re and ^{188}Re , as a potential radiopharmaceuticals, not only for diagnosis but also for therapeutic purposes [18,19].

Modern theoretical calculations, mainly those derived from the applications of density functional theory (DFT) have significantly contributed in the characterization of metal complexes. They have successfully been applied to study very large systems due to their good compromise between computational cost, coverage, and accuracy of results. While diverse theoretical studies dealing with electronic structure of complexes with the center $\{\text{MoOS}_4\}$ have been conducted [20–22], the electronic structure of complexes of type $[\text{VOS}_4]^{2-}$ and $[\text{ReOS}_4]^-$ still remains practically unknown. A DFT study for $[\text{VO}(\text{bdt})_2]^{2-}$ employing the BLYP [23,24] functional and the zero-order regular approximation (ZORA) has been performed. However, to the best of our knowledge $[\text{ReO}(\text{bdt})_2]^-$ has not been studied theoretically.

Herein, we report the assessment of several DFT methods in combination with several basis sets in describing geometry and bond nature for the closed-shell rhenium(V) oxocomplex

* Corresponding author.

E-mail addresses: gancheff@uni-muenster.de, jorge@fq.edu.uy (J.S. Gancheff).

[ReO(bdt)₂][−] and the open-shell vanadium(IV) oxocomplex [VO(bdt)₂]^{2−}. It is our interest to investigate the electronic structure of [VO(bdt)₂]^{2−} and [ReO(bdt)₂][−] and to address issues regarding the nature of their chemical bonds. The results indicated that several density functionals have problems in describing the Re—S bond. In this regard, a study dealing in turn with a test of the best methodology on a different system containing rhenium–sulfur bonds is included.

2. Computational details

All calculations were carried out at the density functional (DFT) level of theory. Geometries were fully optimized in the gas phase in absence of counterion starting from crystallographic data in given symmetry as presented in Fig. 1. [ReO(bdt)₂][−] and [VO(bdt)₂]^{2−} were studied in a singlet (*S* = 0) and doublet (*S* = 1/2) state, respectively. The completely unrestricted formulation was employed for the open-shell system and spin contamination was negligible in all cases. The functionals we tested in this work comprise one generalized gradient approximation (GGA) [24], one *m*-GGA [25], and four hybrid GGA (HGGA) methods [26–31], for which a brief description or their properties is given in Table 1. Two standard basis sets, LANL2DZ and SDD, seven composite ones are employed in this work. They are described in Table 2. In all of them labeled with “LTZ”, light atoms were described with Pople type basis sets [32–36] and the valence electrons for the metal were described using LANL2TZ(f) (a triple- ζ quality basis set), the core electrons being treated through the pseudopotential approximations (ECP) as implemented in LANL2DZ [37,38]. The valence electrons for non-metal in STMIDI were treated with MIDI! [39], those for the metal being described by a basis set (8s7p6d2f1g)/[6s5p3d2f1g] [40–42]. The core electrons were replaced by Stuttgart effective core pseudopotentials [40–43]. The latter have also been employed to replace two inner electrons for C, N, O, 10 inner electrons for S [44], and the core electrons for the metallic centers in the STT basis set. All basis sets take scalar relativistic effects into account, especially important when systems with transition metal atoms are studied [45]. The nature of the stationary point was verified through a vibrational analysis (no imaginary frequencies). Natural bond orbital

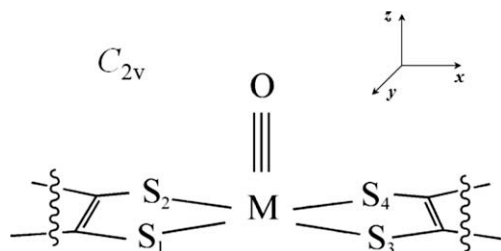


Fig. 1. Coordinative system employed for [Mⁿ⁺O(bdt)₂]^{(n−6)−} [Mⁿ⁺ = V^{IV}, Re^V].

Table 1
Properties of the functionals employed in the calculations.

Functional	Type ^a	X ^b	Refs.
BP86	GGA	0	[23,24]
TPSS	<i>m</i> -GGA	0	[25]
B3LYP	HGGA	20	[24,26,27]
X3LYP	HGGA	21.8	[28]
PBE1PBE	HGGA	25	[29–31]
BH&HLYP	HGGA	50	[27,31]

^a GGA, generalized gradient approximation; *m*-GGA, *meta*-GGA; HGGA, hybrid GGA.

^b X = HF exchange operator (%).

Table 2

Basis sets employed for valence electrons of the complexes studied in this work.

Basis set	Re	S	O	C	H
LTZ631	LANL2TZ(f)	6-31+G [*]	6-31G [*]	6-31G [*]	3-21G [*]
LTZ631+	LANL2TZ(f)	6-31+G [*]	6-31+G [*]	6-31+G [*]	6-31++G ^{**}
LTZ6311	LANL2TZ(f)	6-311+G [*]	6-31+G [*]	6-31+G [*]	3-21G [*]
LTZ6311+	LANL2TZ(f)	6-311+G(2df)	6-311+G [*]	6-311+G [*]	6-31++G ^{**}
LTZ6311++	LANL2TZ(f)	6-311+G(2df)	6-311+G(2df)	6-31+G [*]	6-311++G ^{**}
STT	(8s7p6d2f1g)/[6s5p3d2f1g]	6-31+G [*]	6-31+G [*]	6-31+G [*]	cc-pVTZ
STMIDI	(8s7p6d2f1g)/[6s5p3d2f1g]	MIDI!	MIDI!	MIDI!	MIDI!

(NBO) calculations were performed with the NBO code [46–48] included in the program package Gaussian 03, Rev. D.02 [49], which has been used for all calculations reported in this work.

To make a reasonable comparison between experiment and theory we must use as reference quite precise structural data. However, to the best of our knowledge no gas electron diffraction or microwave spectroscopy data is available for complexes including the Re—S. For this reason we used as reference the crystallographic data available [50,51]. Vibrational corrections were not considered because they are smaller [63] than the deviations between the experimental bonds distances determined with different counterions [50,51]. Indeed, the experimental determinations of the Re—S bond distances differ by as much as 0.015 Å [50,51], whereas the vibrational corrections determined for third-row transition metal complexes by Buhl et al. [63] are in general one order of magnitude smaller. Also, it is important to note that we are interesting in studying very large metal complexes, for which the calculation of vibrational corrections represents a formidable task.

3. Results and discussion

For purposes of structural organization, we have partitioned our discussion of results into subsections dealing in turn with equilibrium geometries and electronic properties of: (i) the closed-shell oxorhenium(V) complex [ReO(bdt)₂][−], (ii) the open-shell oxovanadium(IV) complex [VO(bdt)₂]^{2−}, (iii) we have studied hexanuclear anionic clusters [Re₆S₈X₆]^{4−} (X[−] = Cl[−], Br[−], I[−]) which contain Re—S bonds. This part is aimed to assess the validity of the conclusions drawn from the analysis of (i) and (ii).

3.1. [ReO(bdt)₂][−]

The general features observed in the experimental data [50,51] are well reproduced in the calculations, despite of some large deviation in calculated bond lengths. The presence of the oxo terminal ligand results in the metal center residing 0.7 Å out the plane defined by the four sulfur donor atoms. All the atoms in the C₆S₂ groups remain coplanar with the C—C bond distance about 1.40 Å. In describing Re—S bonds in particular (see Fig. 2), the DFT methods can be grouped into three groups, namely:

- Group 1: B3LYP and X3LYP
- Group 2: BP86, TPSS, and BH&HLYP
- Group 3: PBE1PBE

Deviations of the distance Re—S for the methods of Group 1 are obtained in the range from +0.122 (LANL2DZ) to +0.023 Å (STMIDI). Both methods have serious problems describing this bond. For the methods of Group 2, the deviations range from +0.093 (LANL2DZ) to +0.011 Å (TPSS/STMIDI), giving acceptable overestimated distances (less than +0.02 Å) only for the largest basis sets employed, namely LTZ6311+ and LTZ6311++. The best agreement

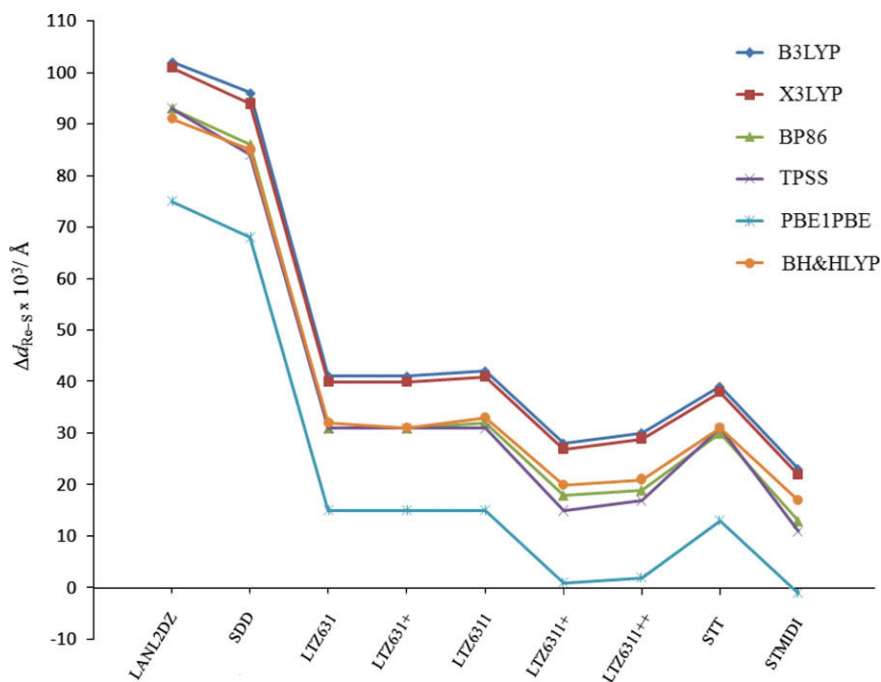


Fig. 2. Difference in the bond distance Re–S between calculated values and the crystallographic result for $[\text{ReO}(\text{bdt})_2]^-$, as obtained by employing several DFT methods.

between experiment and theory is obtained by employing the PBE1PBE method. In effect, employing the latter functional we have obtained the smallest deviations: +0.001 (LTZ6311+) and –0.001 Å (STMDI). However, as observed for the methods of Groups 1 and 2, the results are strongly dependent on the basis sets employed. For the LANL2DZ and SDD basis sets the Re–S are longer than the experimental results by +0.075 and +0.068 Å, respectively. In short, the PBE1PBE method, combined with the MIDI! basis set

and the Stuttgart energy consistent pseudopotentials gives the best description of the Re–S bond length maintaining the computational cost very low.

The performance of the DFT methods to describe the Re–O bond shows a direct dependency on the HF exchange value (X), as can be seen in Fig. 3. On going from the pure GGA (BP86) and m -GGA (TPSS) with non-HF exchange, to the HGGA methods like PBE1PBE (with % $X = 25$), a sensible improvement is observed with

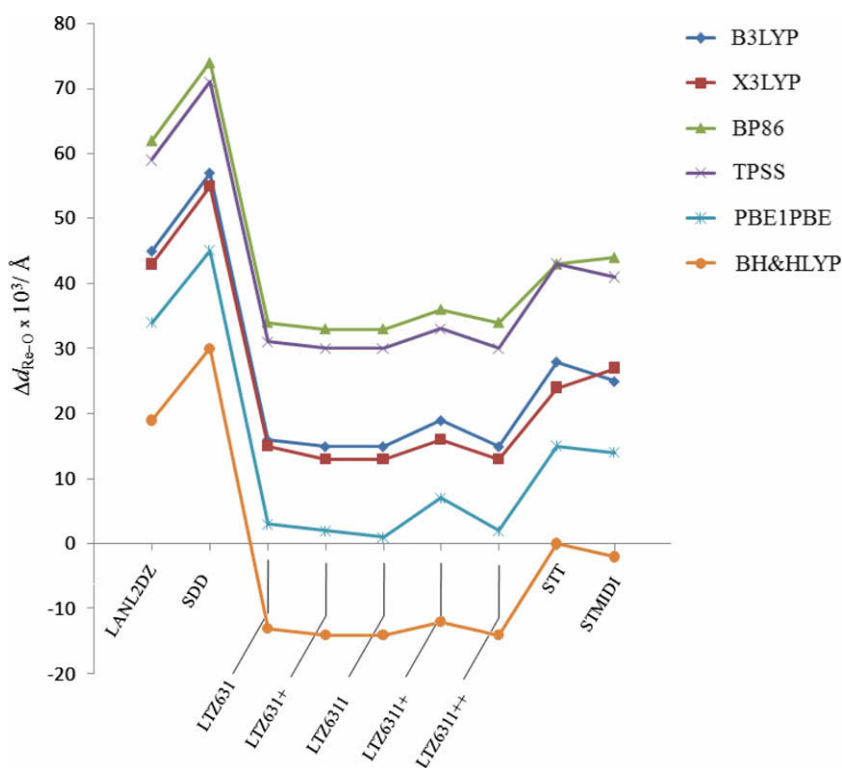


Fig. 3. Difference in the bond distance Re–O between calculated values and the crystallographic result for $[\text{ReO}(\text{bdt})_2]^-$, as obtained by employing several DFT methods.

Table 3

Selected atomic charges from the NPA for $[\text{ReO}(\text{bdt})_2]^-$ in a C_{2v} symmetry employing several DFT methodologies.

Functional	Basis set	Re	O	S
B3LYP	LANL2DZ	+0.638	−0.482	−0.090
	LTZ6311+	+0.709	−0.531	−0.058
	STMIDI	+0.535	−0.472	−0.006
X3LYP	LANL2DZ	+0.628	−0.490	−0.089
	LTZ6311+	+0.709	−0.550	−0.039
	STMIDI	+0.542	−0.477	−0.007
TPSS	LANL2DZ	+0.533	−0.453	−0.068
	LTZ6311+	+0.596	−0.521	−0.014
	STMIDI	+0.431	−0.447	+0.023
BP86	LANL2DZ	+0.491	−0.440	−0.057
	LTZ6311+	+0.547	−0.509	+0.002
	STMIDI	+0.377	−0.429	+0.035
PBE1PBE	LANL2DZ	+0.594	−0.475	−0.079
	LTZ6311+	+0.667	−0.542	−0.028
	STMIDI	+0.493	−0.476	+0.014
BH&HLYP	LANL2DZ	+0.783	−0.526	−0.122
	LTZ6311+	+0.863	−0.589	−0.078
	STMIDI	+0.694	−0.531	−0.035

all basis set. This method in combination with the LTZ6311 basis set leads to a very good estimation of the Re–O distance: 1.664 Å (exp. value of 1.663 Å [50]). An intermediate behavior has been obtained for B3LYP and X3LYP with X of 20% and 21.8%, respectively. In these cases, only those basis sets including LANL2TZ(f) for rhenium give an acceptable deviation less than +0.020 Å. The shortest Re–O bond distances are obtained with BH&HLYP. This fact confirms the idea that when the HF exchange is increased, the Re–O bond distance decreases, in sharp contrast with the results obtained for the Re–S bond. In contrast with the results obtained for the Re–S bond, PBE1PBE/STMIDI does not give the best description of the Re–O bond (deviation of +0.014 Å). In effect, larger basis sets like the LTZ6311++ are necessary to obtain an error similar to the one observed for the Re–S bond when estimated at the PBE1PBE/STMIDI level (around +0.001 Å).

For gaining insight into the knowledge of the bond composition, a natural bond orbital (NBO) study were performed by means of all aforementioned DFT functionals in combination with LANL2DZ, LTZ6311+, and STMIDI. The results of the natural population anal-

ysis (NPA) are presented in Table 3. The calculated charges on rhenium are considerable lower than the formal charge of +5 as a product of a significant electronic density donation from the oxo and the thiolato ligands. The oxo ligand supports NPA charges in the range of −0.429 to −0.589. The variation of the charge separation within the oxo core $[\text{Re}=\text{O}]^{3+}$ has showed dependence on the basis set and in some extension on the HF exchange, as we can appreciate in Fig. 4. The presence of diffuse and polarization functions on non-metallic atoms, like in the LTZ6311+ basis set, leads to an increment in the charge separation for all methods. In general an increase in HF exchange is accompanied with a major charge separation, taken BP86 and BH&HLYP for comparison.

For further understanding of the bond characteristics involving rhenium, a natural bond analysis has been performed (see Table S1). Among the selected methodologies, only those derived from the use of LANL2DZ and STMIDI and BH&HLYP/LTZ6311+ give rise to three natural Re–O bonds, consisting of bonding contributions by one σ and two π bonds [52]. This bond is strongly polarized toward the oxygen atom, the metal contribution to the σ bond going from 27.14% (BH&HLYP/STMIDI) to 29.65% (BP86/STMIDI). The Re–O π bonds are even more polarized: the metal contribution is in all cases less than 23%. This means that the s and particularly the p contribution gives to the Re–O bond character of a donor–acceptor bond. The hybridization at rhenium shows clearly that the d contribution dominates the metal bonding in the σ and π oxo bonds. It is worth to mention that in the π bonds the oxo ligand employs pure or quasi pure p atomic orbitals. The nature of the Re–O bonds is in agreement with the results obtained in previous works regarding analysis of the bonding nature of transition metal oxocomplexes [53–57].

All sulfur donor atoms participate in σ bond and show hybridization at the metal which has mainly d character, while at the sulfur has mainly p character. These results are in good agreement with the ones obtained by Neuhaus et al. [57] for $[\text{ReOX}_4]^-$ ($X^- = \text{F}^-, \text{Cl}^-$). In analogy with the Re–O bond, a strong polarization toward the non-metal in all Re–S bonds was also detected, the contribution of rhenium being less than 25%.

3.2. $[\text{VO}(\text{bdt})_2]^{2-}$

All the geometry optimizations starting from structures with C_{2v} symmetry have reached a minimum (real frequencies). The

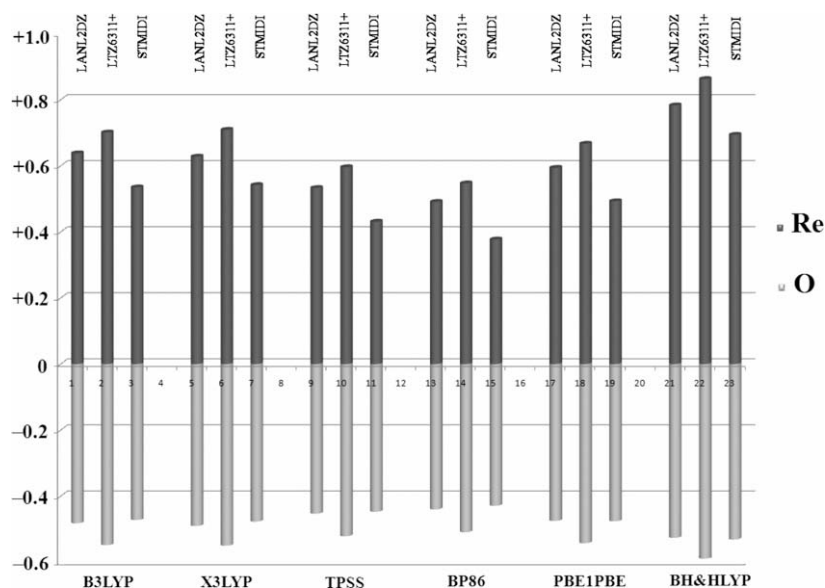


Fig. 4. Charge separation within the oxo core $[\text{Re}=\text{O}]^{3+}$ for $[\text{ReO}(\text{bdt})_2]^-$, as obtained by employing several DFT methods and the natural population analysis (NPA).

optimized geometry (for which non-spin contamination were obtained) shows differences with respect to the crystallographic structure [14]. As expected, this result is in concordance with the calculations performed by Cooney et al. [14], which has been carried out theoretical studies on this system starting from the C_{2v} symmetry. The disagreement between the geometry at the minimum and the crystallographic structure found its explanation in the fact that the counterions (triethylammonium) are disposed in such way, that H-bonds to the oxo ligand via the ammonium proton and to one of the sulfur atoms of the dithiolato ligand are formed. The H-bonding promotes to the four sulfur atoms lying twisted away from being coplanar [14]. Some large deviations in calculated bond lengths are obtained. The oxo ligand occupying the apical position of the square pyramidal coordination geometry forces the metal center to move 0.7 Å out the plane defined by the four sulfur donor atoms. The C_6S_2 groups are essentially planar with the C–C bond distance about 1.40 Å. As can be seen in Fig. 5, the DFT methods behave similarly in describing V–S bonds, their performance being however markedly different to $[ReO(bdt)_2]^-$. Almost all of the DFT methodologies employed have serious problems in describing this bond. The V–S bond length is overestimated by up to +0.118 Å. BP86, TPSS, and PBE1PBE in combination with STMIDI lead to slight deviations of –0.001, +0.002, and –0.003 Å, respectively. These results significantly improve the theoretical deviation of +0.0902 Å calculated by Cooney et al. [14] for the same complex, employing the BLYP functional and treating scalar relativistic effects by the zero-order regular approximation (ZORA) [14].

In the description of the V–S and Re–S bonds, it is to be highlighted an important difference given by the DFT methods employed in this work. In the case of Re–S bond, when larger basis sets (like LTZ6311+) are employed, the estimated bond distance is very similar to the one computed using the STMIDI basis sets. Both results are very close to the experimental value. However, for the V–S bond, only the value calculated by STMIDI is close to the experimental result. In this case LTZ6311+ gives a result +0.040 Å far from the experimental value. Therefore, we expect a poor description of the V–S at the complete basis set limit but a good one for Re–S, confirming the aforementioned bad description of the V–S bond. In short, for the V–S bond it does not seem to be a good choice to extend the basis set.

The performance of the DFT methods to describe the V–O bond shows interesting features; they are presented in Fig. 6. All of the methodologies employed underestimate this bond distance, leading to deviations up to –0.077 Å. When the HF exchange (X) is taken into account on going from BP86 and TPSS to BH&HLYP, a sensible overestimation of the bond is obtained as it is shown in Fig. 6. The pure DFT functionals in combination with LANL2DZ give the best result with deviation of –0.017 Å. However, the PBE1PBE performs rather poorly in the determination of the V–O bond lengths, being one of the worst choices. Indeed, if we compare Fig. 3 (Re–O bond) and Fig. 6 (V–O bond), the poor performance of PBE1PBE becomes evident. The shortest V–O bond distances are obtained with BH&HLYP, which contains the larger amount of HF exchange. This fact is in line, once again, with the idea that when the HF exchange is increased, the V–O bond distance decreases, markedly contrasting with the results obtained for the V–S bond, and similar to the behavior observed for the Re–O bond.

A natural bond orbital (NBO) study was performed for all of the functionals employed in this work in conjunction with the LANL2DZ, LTZ6311+, and STMIDI basis sets. The NPA results are presented in Table 4. Analogous to those previously discussed for rhenium, the donation of electronic density from the oxo and thiolato ligands produces a considerable decrease in the formal charge of +4 on vanadium. The most basic site of the molecule is located on the oxo ligand, the NPA charges ranging from –0.440 to –0.626. The charge separation within the oxo core $[VO]^{2+}$ is presented in Fig. 7. It behaves similar to that calculated for rhenium, the major charge separation is obtained for BH&HLYP/LTZ6311+.

Without exceptions, the results of the bonding nature analysis (Table S3) clearly point to the existence of one σ and two π natural V–O bonds by using all the methodologies. This bond results strongly polarized toward the oxo ligand. The metal contribution to the σ bond is in the range from 25.30% (B3LYP/STMIDI) to 29.37% (BH&HLYP/LANL2DZ). In contrast with that calculated for rhenium, the V–O π and σ bonds are polarized in the same extension. The hybridization at vanadium shows clearly that the d contribution dominates the metal bonding in the σ and π oxo bonds. For the π bonds the oxo ligand employs pure or quasi pure p atomic orbitals. The nature of the V–O bonds is in line with previous works regarding analysis of the bonding nature of transition metal oxocomplexes [53–57]. All sulfur donor atoms participate in σ

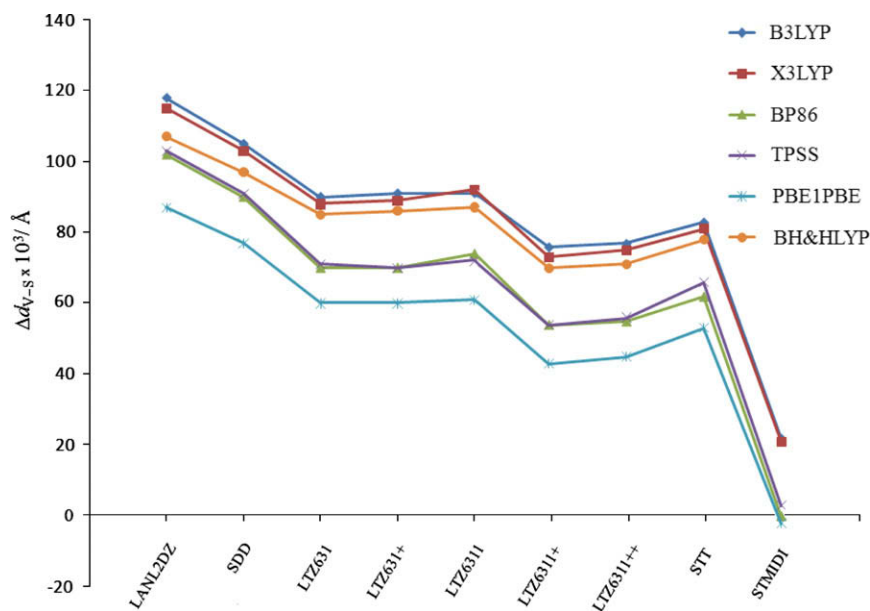


Fig. 5. Difference in the bond distance V–S between calculated values and the crystallographic result for $[VO(bdt)_2]^{2-}$, as obtained by employing several DFT methods.

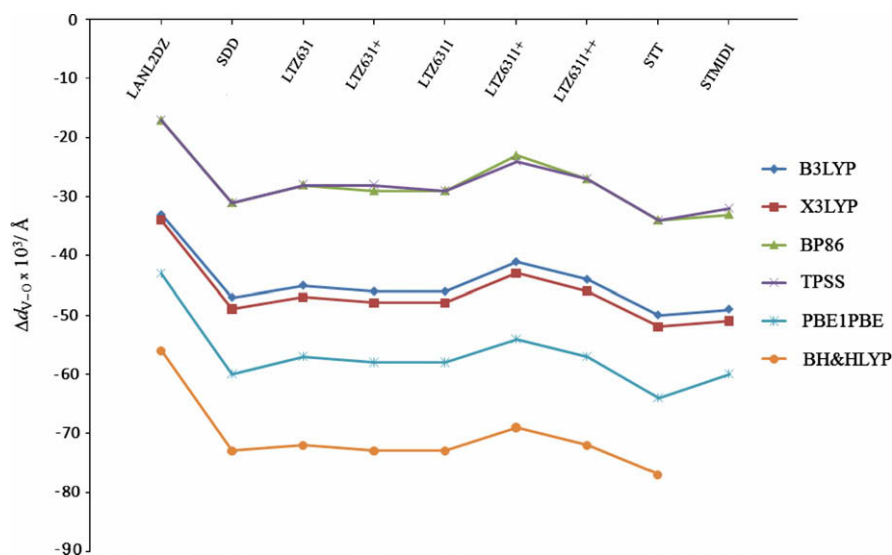


Fig. 6. Difference in the bond distance V–O between calculated values and the crystallographic result for $[\text{VO}(\text{bdt})_2]^{2-}$, as obtained by employing several DFT methods.

Table 4

Selected atomic charges from the NPA for $[\text{VO}(\text{bdt})_2]^{2-}$ in a C_{2v} symmetry employing several DFT methodologies.

Functional	Basis set	V	O	S
B3LYP	LANL2DZ	+0.619	−0.496	−0.248
	LTZ6311+	+0.680	−0.567	−0.199
	STMIDI	+0.580	−0.529	−0.173
X3LYP	LANL2DZ	+0.604	−0.487	−0.248
	LTZ6311+	+0.688	−0.570	−0.200
	STMIDI	+0.585	−0.532	−0.175
TPSS	LANL2DZ	+0.485	−0.455	−0.216
	LTZ6311+	+0.534	−0.532	−0.160
	STMIDI	+0.450	−0.488	−0.134
BP86	LANL2DZ	+0.431	−0.440	−0.202
	LTZ6311+	+0.478	−0.515	−0.141
	STMIDI	+0.386	−0.463	−0.120
PBE1PBE	LANL2DZ	+0.581	−0.489	−0.246
	LTZ6311+	+0.630	−0.558	−0.186
	STMIDI	+0.537	−0.526	−0.154
BH&HLYP	LANL2DZ	+0.747	−0.529	−0.288
	LTZ6311+	+0.867	−0.626	−0.250
	STMIDI	+0.770	−0.610	−0.214

bond. At this point it deserves to be mentioned that none V–S bond was detected obtained by using BH&HLYP/STMIDI. While the hybridization at the non-metal has mainly *p* character, the hybridization at vanadium shows a major *s* character or a major *p* character than in the case of rhenium.

The analysis of the $[\text{ReO}(\text{bdt})_2]^-$ and $[\text{VO}(\text{bdt})_2]^{2-}$ complexes containing the Metal–S bond clearly point to the PBE1PBE method as the best choice to estimate their structural parameters. This result is in good agreement with that obtained by Buhl et al. [63] who studied the performance of several DFT methods in the determination of the structural parameters of third-row transition metal complexes.

3.3. Test case

In this section, we present the results of the study for $[\text{Re}_6\text{S}_8\text{X}_6]^{4-}$ ($\text{X}^- = \text{Cl}^-, \text{Br}^-, \text{I}^-$), as obtained by using PBE1PBE in combination with STMIDI. It is important to note that in the case of bromine and iodine the core electrons were replaced by Stuttgart effective core pseudopotentials. The basis set employed for the lat-

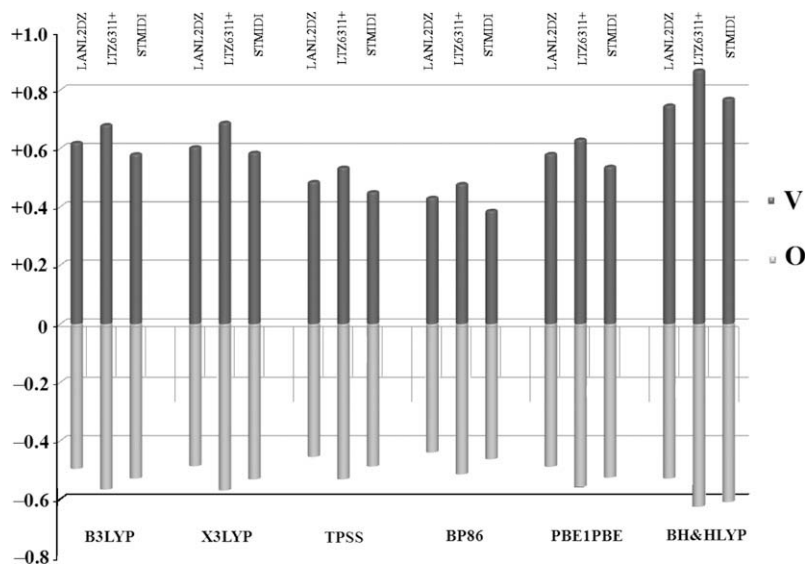


Fig. 7. Charge separation within the oxo core $[\text{VO}]^{2+}$ for $[\text{VO}(\text{bdt})_2]^{2-}$, as obtained by employing several DFT methods and the natural population analysis (NPA).

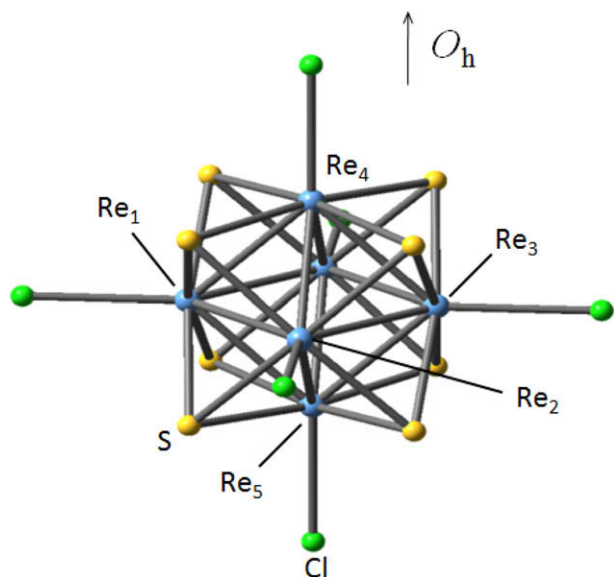


Fig. 8. Optimized geometry of $[\text{Re}_6\text{S}_8\text{Cl}_6]^{4-}$ as obtained by employing PBE1PBE/STMIDI.

ter two was the VTZ basis set which accompanies those pseudopotentials. We have selected this methodology because we are interested in finding a methodology with a rather small computational cost without losing accuracy, which can allow us to study large metal complexes. The results presented in the previous sections indicate that PBE1PBE gives the best structural parameters (with the exception of the V–O bond) for the complex investigated herein. Therefore, such methodology will enable us to study large molecules like double- or triple-stranded helicates containing sulfur donor atoms. For the $[\text{Re}_6\text{S}_8\text{X}_6]^{4-}$ hexanuclear clusters, the metal is presented as rhenium(III). Theoretical DFT studies for these anionic clusters have been performed by Gray et al. [58,59] employing, HF, BLYP, B3LYP, BP86, and B(24.3HF)P86 and by Arratia-Pérez et al. [60]. As discussed in Sections 3.1 and 3.2, PBE1PBE/STMIDI leads to excellent description of Re–S bonds. Although LTZ6311+ leads also to excellent results, its use leads to a sensible higher computational cost than when employing STMIDI. The calculations comprise geometry optimization in the O_h symmetry, for which the singlet state was taken into account. The bond analysis was carried out employing the NBO code. The optimized geometry for $[\text{Re}_6\text{S}_8\text{Cl}_6]^{4-}$ is presented in Fig. 8, while selected geometric parameters for all of the complexes are presented in Table 5. The general trends observed in the experimental data are well reproduced in

the calculation. Calculated bond lengths and angles are in excellent agreement with the values taken from the X-ray diffraction results. In describing intermetallic Re–Re bonds, PBE1PBE/STMIDI underestimates the experimental bond distances by -0.009 , -0.015 , and -0.020 Å for Cl^- , Br^- , and I^- , respectively, although it is worth noticing that it significantly improves the previous estimations [58,59]. For the Re–S bonds, the employed methodology gives the most astonishing agreement notably improving the results reported by Gray et al. [58,59], independent of the employed methodology. The methodology proposed in this work leads to a deviation of only $+0.001$, $+0.004$, and -0.008 Å for Cl^- , Br^- , and I^- , respectively. For the Re–X bonds ($\text{X}^- = \text{Cl}^-$, Br^- , I^-), once again the chosen methodology improves the theoretical results previously reported [58,59]. However, the description is not as good as the ones observed for Re–Re and Re–S. In effect, the errors are quite large, -0.023 , $+0.055$, and $+0.082$ Å, for chlorine and bromine, respectively. However, they are a significantly smaller than the ones reported in Ref. [59].

The results of the natural charges as obtained from the NPA leads to a negative charge on all atoms, namely, $\text{Re}^{-0.119}$, $\text{S}^{-0.037}$, $\text{Cl}^{-0.498}$. It is the product of the charge donation from the four sulfur donor atoms and the halogenide. These results are in line with that reported by Arratia-Pérez et al. [60], which by means of their relativistic population analysis algorithm at the X_α level of theory [61,62], have calculated the charge distribution as follow: $\text{Re}^{-0.21}$, $\text{S}^{-0.16}$, $\text{Cl}^{-0.24}$. In our case, the charge donation coming from the sulfur atoms is more important than from chloride, taking the changes of the charge distribution compared to the formal charge of -2 on sulfur and of -1 on chloride into account.

The results of the bond analysis as obtained from the NBO code are presented in Table 6. All atoms participate in σ bonds. In the case of the intermetallic bond, two slight different bonds were detected: one comprises the so-called “in-plane” rhenium atoms and another one involving “out-plane” metallic center. The former results slight polarized toward one of the rhenium. The hybridization at both atoms results practically the same, for which the d contribution dominates. It is worth mentioning that by means of this basis set, the contribution arising from the f orbitals are slight more important than those arising from the s orbitals. The “out-plane” rhenium–rhenium bond is described as a quasi perfect covalent bond, for which the hybridization shows analogous features to that already discussed for “in-plane” intermetallic bond.

In describing the Re–S bond, analogous features are found in comparison with that discussed for $[\text{ReO}(\text{bdt})_2]^-$. This bond is strongly polarized toward the non-metal, the contribution of rhenium being about 31%. While the hybridization at the metal has mainly d character, at the sulfur atom has mainly p character. In this case the f contribution to the hybridization at rhenium is less

Table 5

Calculated and experimental selected parameters (distances in Å; angles in $^\circ$) in $[\text{Re}_6\text{S}_8\text{X}_6]^{4-}$ ($\text{X}^- = \text{Cl}^-$, Br^- , I^-) in a O_h symmetry singlet state.

Interatom	HF(1) ^a	HF(2) ^a	BLYP ^a	B3LYP(1) ^a	B3LYP(2) ^a	BP86 ^a	B(24.3HF)P86 ^a	PBE1PBE/STMIDI	Exp. ^b
Re–Re	2.6081	2.541	2.6748	2.6442	2.597	2.650	2.619	2.586	2.601
Re–S	2.4880	2.414	2.5346	2.5081	2.435	2.449	2.428	2.404	2.403
Re–Cl	2.5401	2.567	2.5813	2.5486	2.555	2.521	2.496	2.428	2.451
S–Re–Cl								93.1	93.1
Re–Re	2.6070		2.6754	2.6446				2.587	2.596
Re–S	2.4860		2.5325	2.5066				2.401	2.397
Re–Br	2.7087		2.7581	2.7186				2.651	2.596
S–Re–Br	92.0		92.3	92.3				93.2	93.1
Re–Re	2.6110		2.6767	2.6453				2.587	2.607
Re–S	2.4838		2.5311	2.5038				2.400	2.408
Re–I	2.8930		2.9578	2.9070				2.862	2.780
S–Re–I	92.1		92.3	92.3				93.2	93.4

^a (1) refers to the method employed when combined with the Hay–Wadt basis set; (2) idem with the so-called “enhanced basis set” in Ref. [58].

^b $[\text{Re}_6\text{S}_8\text{Cl}_6]^{4-}$ taken from Ref. [57], $[\text{Re}_6\text{S}_8\text{Br}_6]^{4-}$ and $[\text{Re}_6\text{S}_8\text{I}_6]^{4-}$ taken from Ref. [58].

Table 6

Contribution (%) of atomic orbital to selected natural bond orbitals (NBO) between rhenium, sulfur, and chloride in the bond analysis of $[\text{Re}_6\text{S}_8\text{Cl}_6]^{4-}$ in a O_h symmetry employing PBE1PBE/STMIID. ^{a,b,c,d,e,f,g}

Bond		% ns	% np	% (n – 1)d	% (n – 2)f
Re–Re ^{f,g}	In-plane	% Re ₁	% Re ₂		
		60.62	1.23	16.09	76.02
	Out-plane	39.98	4.23	27.32	63.05
		50.41	3.83	26.49	63.86
Re–S					
		49.59	4.23	27.32	63.05
		% Re	% S		
		30.88	17.45	12.27	61.90
Re–Cl					
		69.12	10.97	88.78	0.28
		% Re	% Cl		
		23.39	37.90	2.63	58.77
		76.61	24.12	75.79	0.09

^a $n = 6$ for Re; $n = 3$ for S and Cl.

^b The % of the f orbital corresponds only for the metal.

^c The % of the g orbitals to the hybridization at rhenium is not given.

^d % Re gives the contribution of the bond at the metallic atom; % ns , % np , and % $(n – 1)d$ give the hybridization of the bond.

^e For each bond, in the first and second rows, respectively, the hybridization at Re(1), and Re(2) or at the non-metal are given.

^f For atom assignment, see Fig. 8.

^g “In-plane” rhenium are those in the equatorial plane defined by Re₁, Re₂, and Re₃ (the molecular orientation as showed in Fig. 8); “out-plane” rhenium are Re₄ and Re₅.

important than the s one. The Re–Cl bonds are even more polarized: the metal contribution is about 24%. In this case the hybridization at the metal is dominated by the d contribution, the s contribution being also important but not in the same extension. The contribution coming from the f orbital in this case is residual. The hybridization at the non-metal is dominated by the p contribution.

4. Conclusions

In this work, we reported the assessment of six DFT methods (BP86, TPSS, B3LYP, X3LYP, PBE1PBE, BH&HLYP) in describing structural and electronic properties and also the nature of the chemical bonds for the closed-shell oxocomplex of Re(V) $[\text{ReO}(\text{bdt})_2]^-$ and the open-shell oxocomplex of V(IV) $[\text{VO}(\text{bdt})_2]^{2-}$. Several basis set were employed, in which the inclusion of polarization and diffuse functions, different effective core potentials to describe the inner electrons of the metallic atoms, and the replacement of inner electrons for all atoms for pseudopotentials were taken as variables into account.

For $[\text{ReO}(\text{bdt})_2]^-$, PBE1PBE is found to be the best overall performer in describing Re–S bonds. It is followed by two groups composed in turn of BP86, TPSS, and BH&HLYP, and another one including B3LYP and X3LYP. For the Re–O bonds, the performance has showed a direct dependency of the Hartree–Fock exchange. On going from the pure GGA (BP86) and m -GGA (TPSS) to BH&HLYP, a sensible improvement is obtained, the last method giving raise to the shortest Re–O distance. The NBO analysis shows a charge separation within the oxo core dependent on the basis set and in some extension on the HF exchange. In terms of chemical bond, all sulfur atoms participate in σ bonds strong polarized toward the non-metal, in which the hybridization at the metal has mainly d character and at the non-metal, p character. For the Re–O all DFT method in combination with LANL2DZ and STMIID were able to detect three natural bonds, consisting of bonding contribution of one σ and two π bonds. When combined with LTZ6311+ all methods beside BH&HLYP detect one bond, two lone pair on the oxo ligand being also observed. In the case of $[\text{VO}(\text{bdt})_2]^{2-}$, almost all methodologies

have problem describing the V–S bond. The use of STMIID notably improves the results when combined with all functionals, leading to excellent descriptions of this bond. All methodologies underestimate the V–O bond distance showing an analogous dependence of the performance with the HF exchange as in the case of rhenium. A good improvement of the reported results is obtained with BP86 and TPSS and LANL2DZ. However, in contrast with the results obtained for the Re–O bond, the PBE1PBE method performs rather poorly in the description of the V–O bond. The charge separation within the oxo core behaves similarly to that already discussed for rhenium. Regarding chemical bond analysis, three V–O natural bonds were detected with all methodologies, all of them strong polarized toward the oxo ligand. The hybridization at vanadium shows mainly d character, the p contribution at the non-metal being more important. Once again, one σ bond connecting vanadium and sulfur was detected, strongly polarized toward sulfur.

This work shows that PBE1PBE in combination with STMIID is the best methodology for the study of rhenium and vanadium complexes with thiolato ligands. For rhenium, it also shows the feasibility to expand its range of application to other systems containing Re–S bonds. This methodology therefore is strongly recommended for the study of large transition metal complexes with thiolato ligands.

Acknowledgments

Jorge S. Gancheff thanks the Alexander von Humboldt Foundation for a Postdoctoral fellowship. Pablo A. Denis thanks PEDECIBA-QUIMICA and CSIC for financial support. We also thank Prof. Dr. C. Mück-Lichtenfeld (Universität Münster) for the support regarding the access to the computational resources.

Appendix A. Supplementary data

Supplementary data associated with this article can be found, in the online version, at doi:10.1016/j.theochem.2009.10.020.

References

- [1] R.-M. Olk, B. Olk, W. Dietzsch, R. Kirmse, E. Hoyer, *Coord. Chem. Rev.* 117 (1992) 99.
- [2] P.I. Clemenson, *Coord. Chem. Rev.* 106 (1990) 171.
- [3] J.L. Zuo, F. You, X.Z. You, H.K. Fun, *Polyhedron* 16 (1997) 1465.
- [4] P. Cassoux, L. Valade, H. Kobayashi, A. Kobayashi, R.A. Clark, A.E. Underhill, *Coord. Chem. Rev.* 110 (1991) 115.
- [5] A.T. Coomber, D. Beljonne, R.H. Friend, J.L. Bredas, A. Charlton, N. Robertson, A.E. Underhill, M. Kurmoo, P. Day, *Nature* 380 (1996) 144.
- [6] D. Sellmann, D. Häussinger, F. Knoch, J.M. Moll, *J. Am. Chem. Soc.* 118 (1996) 5368.
- [7] J.C. Fontecilla-Camps, *Structure and mechanism of metalloenzyme active sites*, in: G. Jaouen (Ed.), *Bioorganometallics*, Wiley-VCH Verlag/GmbH & Co. KGaA, 2006, p. 353.
- [8] R.R. Mendel, *Dalton Trans.* (2005) 3404.
- [9] M.K. Johnson, *Prog. Inorg. Chem.* 52 (2004) 239.
- [10] P.M.H. Kroneck, D.J. Abt, Molybdenum and tungsten. Their roles in biological processes, in: A. Siegel, B. Siegel (Eds.), *Metal Ions Biol. Syst.*, M. Dekker, New York, 2002, pp. 369–403.
- [11] R. Hille, *Chem. Rev.* 96 (1996) 2757.
- [12] M.K. Johnson, D.C. Rees, M.W. Adams, *Chem. Rev.* 96 (1996) 2817.
- [13] A. Volbeda, J.C. Fontecilla-Camps, M. Frey, *Curr. Opin. Chem. Biol.* 6 (1996) 804.
- [14] J.J.A. Cooney, M.D. Carducci, A.E. MacElhaney, H.D. Selby, J.H. Enemark, *Inorg. Chem.* 41 (2002) 7086.
- [15] M.M. Abu-Omar, S. Khan, *Inorg. Chem.* 37 (1998) 4979.
- [16] J.H. Espenson, *Coord. Chem. Rev.* 249 (2005) 329.
- [17] J.H. Espenson, *Adv. Inorg. Chem.* 54 (2003) 158.
- [18] B. Noll, C.S. Hilger, P. Leibnitz, H. Spies, *Radiochim. Acta* 92 (2004) 271.
- [19] A. Zablotskaya, I. Segal, S. Germane, I. Shestakova, E. Lukevics, T. Knies, H. Spies, *Appl. Organomet. Chem.* 16 (2002) 550.
- [20] X.B. Wang, F.E. Inscore, X. Yang, J.J.A. Cooney, J.E. Enemark, L.S. Wang, *J. Am. Chem. Soc.* 124 (2002) 10182.
- [21] J.M. Mc Master, D. Carducci, Y.-S. Yang, E.I. Solomon, J.H. Enemark, *Inorg. Chem.* 40 (2001) 687.
- [22] R.L. McNaughton, M.E. Helton, N.D. Rubie, M.L. Kirk, *Inorg. Chem.* 39 (2000) 4386.

- [23] J.P. Perdew, Phys. Rev. B 33 (1986) 8822.
- [24] A.D. Becke, Phys. Rev. A 38 (1988) 3098.
- [25] J. Tao, J.P. Perdew, V.N. Staroverov, G.E. Scuseria, Phys. Rev. Lett. 91 (2003) 146401.
- [26] A.D. Becke, J. Chem. Phys. 98 (1993) 5648.
- [27] C. Lee, W. Yang, R.G. Parr, Phys. Rev. B 37 (1988) 785.
- [28] X. Xu, W.A. Goddard, Proc. Natl. Acad. Sci. USA 101 (2004) 2673.
- [29] J.P. Perdew, K. Burke, M. Ernzerhof, Phys. Rev. Lett. 77 (1996) 3865.
- [30] C. Adamo, V. Barone, J. Chem. Phys. 110 (1999) 6158.
- [31] A.D. Becke, J. Chem. Phys. 98 (1993) 1372.
- [32] R. Krishnan, J.S. Binkley, R. Seeger, J.A. Pople, J. Chem. Phys. 72 (1980) 650.
- [33] P.C. Hariharan, J.A. Pople, Theor. Chim. Acta 28 (1973) 213.
- [34] M.M. Francl, W.J. Pietro, W.J. Hehre, J.S. Binkley, M.S. Gordon, D.J. DeFrees, J.A. Pople, J. Chem. Phys. 77 (1982) 3654.
- [35] J.S. Binkley, J.A. Pople, W.J. Hehre, J. Am. Chem. Soc. 102 (1980) 939.
- [36] M.S. Gordon, J.S. Binkley, J.A. Pople, W.J. Pietro, W.J. Hehre, J. Am. Chem. Soc. 104 (1982) 2797.
- [37] P.J. Hay, W.R. Wadt, J. Chem. Phys. 82 (1985) 299.
- [38] L.E. Roy, P.J. Hay, R.L. Martin, J. Chem. Theory Comput. 4 (2008) 1029.
- [39] S. Huzinaga, J. Andzelm, M. Klobukowski, E. Radzio-Andzelm, Y. Sakai, H. Tatewaki, in: Gaussian Basis Sets for Molecular Calculations, Elsevier, Amsterdam, 1984.
- [40] M. Dolg, U. Wedig, H. Stoll, H. Preuss, J. Chem. Phys. 86 (1987) 866.
- [41] J.M.L. Martin, A. Sundermann, J. Chem. Phys. 114 (2001) 3408.
- [42] D. Andrae, U. Häussermann, M. Dolg, H. Stoll, H. Preuss, Theor. Chim. Acta 77 (1990) 123.
- [43] A. Bergner, M. Dolg, W. Kuechle, H. Stoll, H. Preuss, Mol. Phys. 80 (1993) 1431.
- [44] P. Pyykkö, The Effect of Relativity in Atoms, Molecules and the Solid State, Plenum, New York, 1990.
- [45] J.P. Foster, F. Weinhold, J. Am. Chem. Soc. 102 (1980) 7211.
- [46] A.E. Reed, F. Weinhold, J. Chem. Phys. 83 (1985) 1736.
- [47] A.E. Reed, R.B. Weinstock, B. Weinhold, J. Chem. Phys. 83 (1985) 735.
- [48] A.E. Reed, L.A. Curtis, F. Weinhold, Chem. Rev. 88 (1988) 899.
- [49] M.J. Frisch, G.W. Trucks, H.B. Schlegel, G.E. Scuseria, M.A. Robb, J.R. Cheeseman, J.A. Montgomery Jr., T. Vreven, K.N. Kudin, J.C. Burant, J.M. Millam, S.S. Iyengar, J. Tomasi, V. Barone, B. Mennucci, M. Cossi, G. Scalmani, N. Rega, G.A. Petersson, H. Nakatsuji, M. Hada, M. Ehara, K. Toyota, R. Fukuda, J. Hasegawa, M. Ishida, T. Nakajima, Y. Honda, O. Kitao, H. Nakai, M. Klene, X. Li, J.E. Knox, H.P. Hratchian, J.B. Cross, V. Bakken, C. Adamo, J. Jaramillo, R. Gomperts, R.E. Stratmann, O. Yazyev, A.J. Austin, R. Cammi, C. Pomelli, J.W. Ochterski, P.Y. Ayala, K. Morokuma, G.A. Voth, P. Salvador, J.J. Dannenberg, V.G. Zakrzewski, S. Dapprich, A.D. Daniels, M.C. Strain, O. Farkas, D.K. Malick, A.D. Rabuck, K. Raghavachari, J.B. Foresman, J.V. Ortiz, Q. Cui, A.G. Baboul, S. Clifford, J. Cioslowski, B.B. Stefanov, G. Liu, A. Liashenko, P. Piskorz, I. Komaromi, R.L. Martin, D.J. Fox, T. Keith, M.A. Al-Laham, C.Y. Peng, A. Nanayakkara, M. Challacombe, P.M.W. Gill, B. Johnson, W. Chen, M.W. Wong, C. Gonzalez, J.A. Pople, Gaussian 03 Rev. D.2, Gaussian Inc., Wallingford, CT, 2004.
- [50] W. Clegg, Acta Crystallogr. C 44 (1988) 172.
- [51] R. Hübener, U. Abram, Acta Crystallogr. C 49 (1993) 1068.
- [52] By using LTZ6311+ in combination with some DFT functionals, one σ Re–O bond is detected. Therefore we decided to test the performance of all basis set with PBE1PBE, for which the best geometric results are obtained. In some cases (see Table S2) the two π Re–O bonds (mentioned in Section 3.1) are labeled as lone pair on the oxo ligand, for which a delocalization *mainly* into the antibonding Re–S bonds is observed (with an associated stabilization energy ΔE_{ij} of about 14 kcal/mol, taken PBE1PBE/LTZ6311+ as example).
- [53] J.S. Gancheff, R. Albuquerque, A. Guerrero-Martínez, T. Pape, L. De Cola, F.E. Hahn, Eur. J. Inorg. Chem. (2009) 4043.
- [54] B. Machura, J. Kusz, D. Tabak, R. Kruszynski, Polyhedron 28 (2009) 493.
- [55] B. Machura, M. Jaworska, P.J. Lodowski, J. Mol. Struct. (THEOCHEM) 766 (2006) 1.
- [56] P. Pyykkö, S. Riedel, M. Patzschke, Chem. Eur. J. 11 (2005) 3511.
- [57] A. Neuhaus, A. Veldkamp, G. Frenking, Inorg. Chem. 33 (1994) 5278.
- [58] T.G. Gray, C.M. Rudzinski, E.E. Meyer, D.G. Nocera, J. Phys. Chem. A 108 (2004) 3238.
- [59] T.G. Gray, C.M. Rudzinski, E.E. Meyer, R.H. Holm, D.G. Nocera, J. Am. Chem. Soc. 125 (2003) 4755.
- [60] R. Arratia-Pérez, L.J. Hernández-Acevedo, Chem. Phys. 110 (1999) 2529.
- [61] R. Arratia-Pérez, D.A. Case, J. Chem. Phys. 79 (1983) 4939.
- [62] R. Arratia-Pérez, L. Hernández-Acevedo, L. Alvarez-Thon, J. Chem. Phys. 108 (1998) 5795.
- [63] M. Buhl, C. Reimann, D.A. Pantazis, T. Bredow, F. Neese, J. Chem. Theory Comput. 4 (2008) 1449.